Aalborg Universitet

AALBORG UNIVERSITY
DENMARK

Does microplastic analysis method affect our understanding of microplastics in the environment?

Liu, Yuanli; Prikler, Bence; Bordós, Gábor; Lorenz, Claudia; Vollertsen, Jes

Published in:
Science of the Total Environment

DOI (link to publication from Publisher):
10.1016/j.scitotenv.2023.166513

Creative Commons License
CC BY 4.0

Publication date:
2023

Document Version
Publisher's PDF, also known as Version of record

Link to publication from Aalborg University

Citation for published version (APA):
Liu, Y., Prikler, B., Bordós, G., Lorenz, C., & Vollertsen, J. (2023). Does microplastic analysis method affect our understanding of microplastics in the environment? *Science of the Total Environment*, *902*, Article 166513. https://doi.org/10.1016/j.scitotenv.2023.166513

General rights
Copyright and moral rights for the publications made accessible in the public portal are retained by the authors and/or other copyright owners and it is a condition of accessing publications that users recognise and abide by the legal requirements associated with these rights.

- Users may download and print one copy of any publication from the public portal for the purpose of private study or research.
- You may not further distribute the material or use it for any profit-making activity or commercial gain
- You may freely distribute the URL identifying the publication in the public portal -

Take down policy
If you believe that this document breaches copyright please contact us at vbn@aub.aau.dk providing details, and we will remove access to the work immediately and investigate your claim.

Science of the Total Environment 902 (2023) 166513

Contents lists available at ScienceDirect

Science of the Total Environment

journal homepage: www.elsevier.com/locate/scitotenv

Does microplastic analysis method affect our understanding of microplastics in the environment?

Yuanli Liu [a,*], Bence Prikler [b,c], Gábor Bordós [b], Claudia Lorenz [a,d], Jes Vollertsen [a]

[a] Department of the Built Environment, Aalborg University, Thomas Manns Vej 23, 9220 Aalborg, Denmark
[b] Eurofins Analytical Services Hungary Ltd., 6. Anonymus st., Budapest 1045, Hungary
[c] Institute of Aquaculture and Environmental Safety, Hungarian University of Agriculture and Life Sciences, 2100 Gödöllő, Hungary
[d] Department of Science and Environment, Roskilde University, 4000 Roskilde, Denmark

HIGHLIGHTS

- Two methodologies led to different MP abundance and MP mass estimates.
- MP isolation process decides the recovery of MPs from the environment.
- Optical substrates affect MP size and mass estimates.
- MP analysis results differed with different analytical technique settings.
- All three individual steps contribute to the conflict of the MP numerical result.

GRAPHICAL ABSTRACT

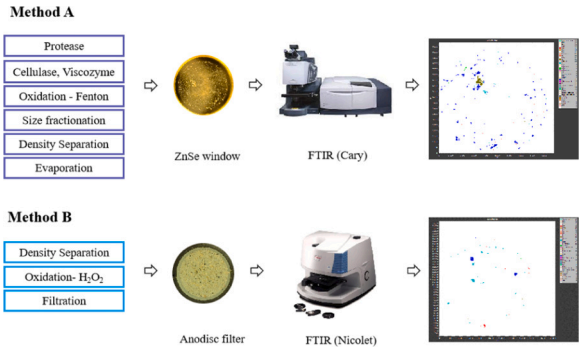

ARTICLE INFO

Editor: Damià Barceló

Keywords:
Microplastics
Methodological approaches
Comparisons
FTIR analysis
Microplastic isolation

ABSTRACT

Two analytical methods – both in active use at different laboratories – were tested and compared against each other to investigate how the procedure influences microplastic (MP) detection with micro Fourier Transform Infrared Spectroscopy (μFTIR) imaging. A representative composite water sample collected from the Danube River was divided into 12 subsamples, and processed following two different methods, which differed in MP isolation procedures, the optical substrate utilized for the chemical imaging, and the detection limit of the spectroscopic instruments. The first instrument had a nominal pixel resolution of 5.5 μm, while the second had a nominal resolution of 25 μm. These two methods led to different MP abundance, MP mass estimates, but not MP characteristics. Only looking at MPs > 50 μm, the first method showed a higher MP abundance, namely 418–2571 MP m^{-3} with MP mass estimates of 703–1900 μg m^{-3}, while the second method yielded 16.7–72.1 MP m^{-3} with mass estimates of 222–439 μg m^{-3}. Looking deeper into the steps of the methods showed that the MP isolation procedure contributed slightly to the difference in the result. However, the variability between individual samples was larger than the difference caused by the methods. Somewhat sample-dependent, the use of two different substrates (zinc selenide windows versus Anodisc filters) caused a substantial difference between results. This was due to a higher tendency for particles to agglomerate on the Anodisc filters, and an 'IR-halo' around particles on ZnSe windows when scanning with μFTIR. Finally, the μFTIR settings and nominal resolution

* Corresponding author.
E-mail address: yuanlil@build.aau.dk (Y. Liu).

https://doi.org/10.1016/j.scitotenv.2023.166513
Received 26 June 2023; Received in revised form 21 August 2023; Accepted 21 August 2023
Available online 22 August 2023
0048-9697/© 2023 The Authors. Published by Elsevier B.V. This is an open access article under the CC BY license (http://creativecommons.org/licenses/by/4.0/).

caused significant differences in identifying MP size and mass estimate, which showed that the smaller the pixel size, the more accurately the particle boundary can be defined. These findings contributed to explaining disagreements between studies and addressed the importance of harmonization of methods.

1. Introduction

Microplastics (MPs) are particles between 1 μm and 5 mm in size, made from or containing significant amounts of manmade or man-modified polymers. They received much attention over the last decade due to their potential adverse effects on biota through bio-uptake and their potential to enter the food web (McIlwraith et al., 2021; Huang et al., 2021; Khalid et al., 2021). The risk of impacting humans via food, drink, and air (Rahman et al., 2021) has further contributed to this attention. MPs have been studied in many environments, for example, terrestrial systems (Rezaei et al., 2022; Corradini et al., 2021), rivers (Yin et al., 2022; Zhang et al., 2022), lakes (Bertoldi et al., 2021; Molazadeh et al., 2023; Xiong et al., 2022), potable water (Bäuerlein et al., 2022; Nizamali et al., 2022), and marine systems (Eo et al., 2021; Simon-Sánchez et al., 2022; Yuan et al., 2022). The bulk of the studies were conducted in the marine environment, while studies on rivers, which are the focus of the present study, have been intensified recently, partly because they convey MPs to the marine environment (Blettler et al., 2018).

Quantification of MPs in complex environmental systems has long been challenged by a lack of method harmonization (Lusher et al., 2020; Primpke et al., 2020a; van Mourik et al., 2021), which has led to discrepancies between results. One cause for poor comparability between studies lies in differences in MP extraction procedures and analytical techniques.

After sampling, proper sample preparation is needed because of the presence of organic and inorganic materials, which might lead to misidentification (González et al., 2016). Hence, some pre-treatment must be used to remove natural organic material and inorganic particles. One way to separate MPs and organic material is to manually remove organic particles after drying the sample (González et al., 2016). Another way is oxidation, which achieves a more thorough removal of natural organic material. Various concentrations of hydrogen peroxide (10–35 %) and temperatures (20–100 °C) have been used here (Thomas et al., 2020; Phuong et al., 2021). High temperatures will, however, also affect some plastics, and are hence not advisable. Hydrogen peroxide oxidation alone will only remove part of the organic matter, and enzymatic digestion is hence commonly included to break down specific substances (Löder et al., 2017). Density separation is widely used to remove inorganic particles, applying solutions of chemicals such as sodium chloride (NaCl) (Lin et al., 2018), sodium iodide (NaI) (Katsumi et al., 2022), zinc chloride ($ZnCl_2$) (Jiang et al., 2019; Liu et al., 2019a), sodium polytungstate (SPT) (Weber and Kerpen, 2022), and lithium metatungstate (Eo et al., 2019). The density of the solution is typically 1.2–1.8 g cm^{-3} (Tirkey and Upadhyay, 2021). As most plastics are lighter than most inorganic particles, this leads to density differences by which plastics can be separated from inorganic particles.

It is worth mentioning that some studies applied both organic matter digestion and density separation (Wang et al., 2020), while some studies used only one of them (Zhou et al., 2020). This outlines some major differences in common sample preparation procedures. In practice, the differences between procedures are even larger, leading to significant differences in extraction efficiencies, recovery rates, and the amount of residual material, which can hamper chemical analysis (Isobe et al., 2019).

Upon sample preparation, extracts are analysed by a variety of analytical techniques, including FTIR (Fourier-transform infrared) spectroscopy, Raman spectroscopy, Pyrolysis GC–MS, etc. (Huang et al., 2023; Prepilkova et al., 2022; Primpke et al., 2020a). FTIR spectroscopy, the approach used in the present study, can be divided into two main groups: approaches that target particles one by one, and approaches that create hyperspectral images, which are then interpreted (Primpke et al., 2017a; Valls-Conesa et al., 2023). The former is primarily utilized in the form of attenuated total reflectance (ATR) FTIR, a contact-based technology that demands crystal cleaning after each analysis, causing time inefficiencies (Song et al., 2015). Conversely, the latter technique, where hyperspectral imaging is mainly performed in transmission mode, demonstrates high efficiency in detecting small microplastics (MPs) (Corami et al., 2020; Kirstein et al., 2021; Possenti et al., 2021; Ye et al., 2022). Consequently, the second method was selected in this study. The extract, or a sub-sample here of, is transferred to an IR-suited substrate on which it is scanned. Substrates are either IR-transmissive filter membranes, IR-transmissive windows, or IR-reflective slides. Research on the pros and cons of different substrates is currently limited. Many researchers prefer filters as it limits the chemical residue. Many have used aluminium oxide membranes (Anodisc, Whatman) and found they work well within the spectral range from 3800 to 1200 cm^{-1} (Löder et al., 2015). The limited spectral range is, however, a drawback, and silicon membranes have been proposed to circumvent this issue (Kappler et al., 2015). While the spectral range benefit is obvious, silicon membranes are still not widely used. Another way to get around the limited spectral range is using IR-transmissive windows, such as done by e.g., Simon et al. (2018). Windows, on the other hand, have the drawback that the extract must be free of dissolved organic compounds, which otherwise can interfere with the analysis.

Going further into the FTIR hyperspectral imaging, which is the technology chosen for the present work, two main technologies are in use: Those using 2-dimensional focal plane array (FPA) detectors versus those using linear array (LA) detectors. The FPA detector creates an n × n array of spectra, typically with $n = 16$, 32, 64, 128, or 256. A linear array creates a 1 × n array of spectra, often with $n = 16$. The detectors are constructed differently and hence have different pros and cons. Both detectors create hyperspectral maps where each pixel is represented by an FTIR-spectrum. The spatial resolution depends on the instrument and its settings. Interpreting the images, which sometimes consist of quite many individual spectra pixels, requires an automated approach. As an example, Kirstein et al. (2021) analysed approx. 9.4 million spectra per hyperspectral image. This can be done in several ways, typically based on some type of machine learning (Primpke et al., 2020b; Wander et al., 2020).

However, FTIR in transmission mode is limited in identifying thick MPs. Hence, these large MPs are often analysed with ATR-FTIR, which can generate high-quality spectra that remain unaffected by particle thickness. However, it does require a manual pre-sorting of potential MPs, followed by individual ATR-FTIR analysis, again leading to extended analysis time.

The above illustrates that the variation in MP analysis approaches is quite large and consists of quite many elements, which all can affect the outcome. Making a comprehensive comparison of all possible variations seems insurmountable. Instead, the present study takes a pragmatic approach by comparing two representative analytical pipelines which are in place and routinely used by the two laboratories participating in this study. One at Aalborg University, Denmark, and one at Eurofins Analytical Services, Hungary. It investigates the impact of two different MP isolation procedures, two different IR scanning substrates, and two different FTIR microscopes. The pipelines were tested on artificially spiked water samples and on environmental samples from the Danube River.

2. Materials and methods

2.1. Sampling

The sampling was done in Budapest, 47.561 N, 19.070E, in the Danube River, Europe's second-longest river (2857 km) after the Volga and one of its most important water systems (Mănoiu and Crăciun, 2021). To ensure a representative river water sample, samples were collected by on-site pressurized fractionated filtration (by pump) on four occasions between 15th October and 29th November 2021. There were at least 10 days kept between consecutive samplings. The filtration apparatus applied three stainless steel filters coupled in series (300, 100, and 50 μm) (Bordós et al., 2021), collecting in total (during the four samplings) 14.5 m^3 of water. Upon collection, the material from all filters and all samples were mixed into one composite sample. Additionally, Danube River water (around 5 L) was collected into glass bottles during each sampling to be used for recovery tests.

The particles from the composite samples were transferred from the filters into a 2 L beaker, and filtered through a 50 μm sieve, resulting in a total concentrated volume of approx. 1 L. The concentrate was divided into 12 subsamples by taking aliquots of 5 mL while stirring the sample, until all concentrate was divided. The subsamples were divided into 4 groups (Fig. 1). Three were processed following a method developed at Aalborg University (Method A); three were processed following a method developed at former Wessling Hungary Kft., now Eurofins Analytical Services Hungary Kft (Method B); three were used to conduct recovery tests on Method A; while the remaining three were used to conduct recovery tests on Method B (Fig. 1).

2.2. MP isolation procedures

2.2.1. Method A

Method A included multiple enzymatic and oxidative steps using a 10 μm stainless steel filter between steps (Rist et al., 2020). In short, the sample was first incubated with protease and cellulase. After that, a Fenton oxidation was done to remove the remaining organic matter, followed by a size fractionation with a 500 μm sieve. The particles >500 μm were dried for analysis, and the fraction containing small particles <500 μm went to density separation with zinc chloride at 1.70–1.80 g cm^{-3} to remove inorganic particles. The extracted samples were concentrated, stored in 10 mL vials, evaporated, and finally filled with 5 mL of 50 % ethanol to achieve a known reference volume. The extracts were homogenized on a vortex mixer, subsamples taken with a disposable glass capillary pipette (50/100 μL) and deposited on Ø 13 × 2 mm zinc selenide (ZnSe) windows (Crystran, UK) held in a compression cell (Pike Technologies, USA). The windows were dried at 50 °C and visually inspected under a stereo microscope to check if they were sufficiently loaded by particles or more aliquots had to be deposited for the FTIR scan. Three windows were prepared and analysed for each sample.

2.2.2. Method B

Method B included density separation and oxidation (Mári et al., 2021). A small-volume glass separator developed by Eurofins Analytical Services Hungary (Mári et al., 2021) was employed for density separation with zinc chloride (1.60–1.70 g cm^{-3}) and the floating part oxidized with hydrogen peroxide (30 %) on a laboratory hot plate at 80 °C for 1 h at 450 rpm without any catalyst. Then the whole sample was filtered onto Whatmann Anodisc aluminium oxide membrane filters (Ø 25 mm; pore size 0.2 μm, GE Healthcare, United Kingdom).

2.3. MP identification

The identification of MPs in the concentrates for both methods was conducted by micro–FTIR spectroscopy (μFTIR). However, the detectors, manufacturers, and sample substrates differed.

2.3.1. MP identification by Method A

The ZnSe windows of Method A were scanned in transmission mode

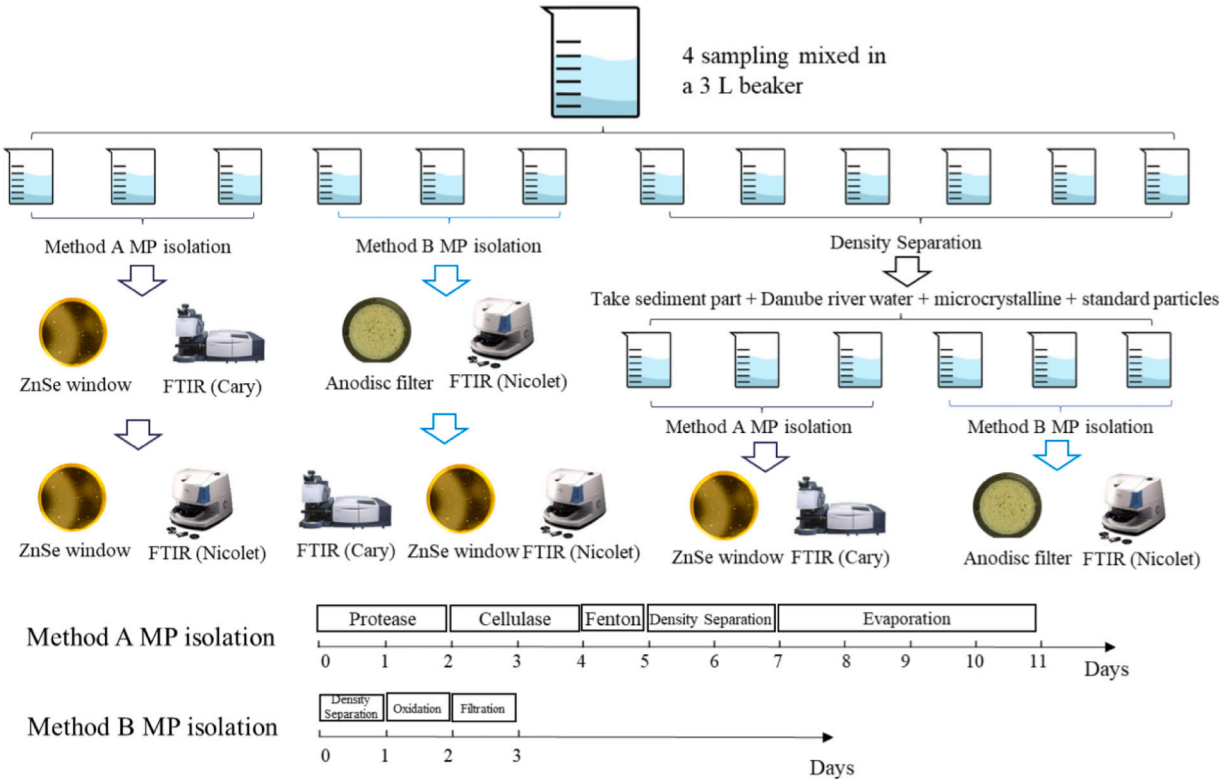

Fig. 1. Diagram of MP detection procedure (Mári et al., 2021; Rist et al., 2020).

at a pixel resolution of 5.5 μm using a Cary 620 FTIR microscope (Cary FTIR) equipped with a Cary 670 IR spectrometer (Agilent Technologies). The microscope used a 15× Cassegrain objective and a 128 × 128 FPA (Mercury-Cadmium-Telluride) imaging detector. The image was created by 30 co-added scans per sample, while the background was acquired by 120 co-added scans. The spectral resolution was 8 cm^{-1} and the wavenumber range 3750–850 cm^{-1}. A single scan of the entire active surface at these settings took around 5 h, resulting in a total of 15 h of scan time for the 3 windows.

All larger particles (>500 μm) were selected, and further imaged using a stereoscopic microscope (ZEISS, SteREO Discovery.V8) with Axiocam 105 color camera and max. 8× magnification. Then, the selected MPs were analysed with a Cary 630 FTIR from Agilent Technologies equipped with a diamond attenuated total reflection (ATR) and the spectra were interpreted with the software OMNIC 8.2.0.387 (Thermo Fisher Scientific Inc., version 1). The software ZenCore (Zen2Core SP1 from ZEISS) was used to quantify the particle's area, minimum, and maximum Feret diameter (Chand et al., 2021).

2.3.2. MP identification by method B

The Anodisc membranes of Method B were placed on the top of a CaF_2 window and scanned in transmission mode at a pixel resolution of 25 μm by a Thermo Scientific Nicolet iN10MX FTIR microscope (Nicolet FTIR) using a 15× Cassegrain objective and a 2 × 8 (Mercury-Cadmium-Telluride) linear detector. The spectral resolution was 8 cm^{-1} and 4 scans were co-added per pixel, covering the wavenumber range 4000–1250 cm^{-1}. At these settings, analysing the entire active surface of one such membrane took around 10 h.

2.4. Comparing individual steps of Method A and B

2.4.1. MP isolation

To explore the effect of the MP isolation procedures and the replicability of the methodology, recovery experiments were conducted. An artificial matrix was prepared to simulate the analysed samples. It comprised: Bulk Danube River water (1 L), 50 mg microcrystalline cellulose (MCC, Sigma-Aldrich Corporation), and sediment from the density separation of subsamples described in Section 2.1. Danube water (Section 2.1) was not MP free, and the MP background concentration hence calculated after the analysis of the environmental subsamples (Section 2.1); i.e., the measured Danube water concentration was subtracted from the recovery results when calculating recovery rates. MCC was added to better model Danube water with higher suspended solid concentrations experienced during previous sampling campaigns (Mári et al., 2021).

Four different types of MP standard particles (20 particles of each type), having different shapes (fragment and fluorescent spherical), polymer types (polyethylene (PE) and polyethylene terephthalate (PET)), and densities (0.95–1.37 g cm^{-3}) (Table 1), were selected and spiked into 1 L artificial matrix. To better represent environmentally occurring MPs (Bannick et al., 2019), the particles were incubated for two weeks at room temperature and moderate stirring in Danube River water. Three such spiked samples were processed by Method A, and three by Method B. After sample preparation, the samples were filtered onto steel filters (Method A) or Anodisc filters (Method B). MPs were initially counted under an optical microscope (Dino-Lite Edge AM4115TL, 10-140× magnification) illuminated with UV light (OP UV LED, 365 nm) to identify beads. After the quick recovery measure of fluorescently labeled standard beads, samples were analysed by μFTIR to determine the recovery of fragments as well. Because there is an overlap in the size range between spherical PE (90–106 μm) and fragment PE (100–300 μm), all PE particles from 90 to 300 μm were selected during recovery analysis with the FTIR. This included both spherical and fragment PE. To calculate the recovery for fragment PE, the number of PE beads identified by UV light was subtracted from the whole PE count. As for the fragment PET, only particles from 100 to 300 μm were selected during recovery analysis with the FTIR, as that was the size range of standard PET used.

Table 1
Physical parameters of the standard MPs particles used for spiking.

Microplastics	Color	Density (g cm^{-3})	Diameter	Shape
PE*	Fluorescent red	1.2	90–106	Spherical
PE*	Fluorescent blue-green	0.98	90–106	Spherical
PE*	White	0.95	100-300	Fragment
PET**	Blue	1.37	100-300	Fragment

Spheres are coming from Cospheric, and fragments were made by cryomilling, which is detailed in Bordós et al., 2021.
* PE – Polyethylene.
** PET – polyethylene terephthalate.

2.4.2. Optical substrates

To explore the effect of substrates, same samples were deposited on both ZnSe window and Anodisc filter. In summary, Method B samples were detected on both Anodisc filters and ZnSe windows, and analysed by the Cary FTIR. First, Method B samples were filtered on Anodisc filters, and analysed by the Cary FTIR. Then the Anodisc filters with samples were placed in three beakers (one per filter) with 50 % EtOH and sonicated for 5 min, separately. The particles on the Anodisc filter were flushed into the beaker and evaporated into 10 mL vials, upon which 5 mL 50 % ethanol was added. After that, subsamples (12–14 %) were deposited on ZnSe windows and scanned by the Cary FTIR.

2.4.3. FTIR settings

To explore the effect of FTIR settings, same samples using same substrates were analysed by FTIR with different settings. In detail, three windows loaded with Method A samples and another three windows loaded with Method B samples were scanned by both the Nicolet and the Cary FTIR.

2.5. Contamination and quality control

Cotton lab coats and nitrile gloves were worn to minimize contamination during sample preparation. All work was done in a Scan-Laf Fortuna Clean Bench (Labogene), and the samples were covered with aluminium foil during the whole procedure. For Method A, all glassware and filters were muffled at 500 °C for 3 h. Chemicals were filtered through 0.7 μm glass fibre filters before use. For Method B, glassware was flushed with filtered water before use. Some contamination was though unavoidable, and three blanks were conducted for each method to assess its magnitude. Blanks were analysed using water filtered through 0.7 μm glass fibre filters and following the same procedures as the samples.

The limit of detection (LOD) and limit of quantification (LOQ) were calculated from the blank values. In line with recommendations by the Association of Official Agricultural Chemists (AOAC International), LOD was defined as the mean of blanks plus 3.3 times the standard deviation of blanks, and LOQ was defined as the mean of blanks plus 10 times the standard deviation of blanks (Horton et al., 2021).

2.6. Data analysis

The hyperspectral images created by the μFTIR imaging were analysed with the software siMPle (Primpke et al., 2020b). siMPle was created in a collaboration between Aalborg University, Denmark (Liu et al., 2019b) and Alfred Wegener Institute, Germany (Primpke et al., 2017b). It compares each pixel of the hyperspectral image to a reference library and creates 2D particle images based here on. It can run with two analytical pipelines, where the current study used the one described in Liu et al. (2019a). Detailed information on the library and applied

thresholds is given in Table S1. The outcome of the analysis is a list of particles (plastics as well as non-plastics) with associated morphological parameters and polymer types. Particle mass is estimated according to Simon et al. (2018), that is, from the volume of the equivalent ellipsoid and the specific density of the polymer. In short: The measured area of the particle's 2-dimensional projection and its maximum Feret diameter (its length) is used to calculate the width of the equivalent ellipse. The 3rd dimension of the equivalent ellipsoid is estimated as 0.6 times the width of the equivalent ellipse. This yields a volume estimate, which is used to estimate mass by multiplying it with the density of the particle's material type. Fibers were defined as MPs where the ratio between major and minor Feret diameters was larger than 3 (Cole, 2016).

3. Results and discussion

3.1. Comparison of MP results

3.1.1. Blanks

MPs of six different polymer types were detected in the blanks: acrylates, polyethylene (PE), polyester, polypropylene (PP), polystyrene (PS), and polyurethane (PU) (Fig. 2(a)). Among these, only PE was found in Method B blanks, while all were found in Method A blanks. It is worth mentioning that more particles were detected in Method A blanks than in Method B blanks (Fig. 2(a)), while the average estimated mass of MPs in Method B blanks (6.9 ± 11.5 mg) was higher than in Method A blanks (0.4 ± 0.3 mg) (Fig. 2(b)). The higher mass observed in Method B primarily came from a single large PE particle in one of the three blanks. Consequently, there is significant uncertainty associated with the mass estimation in Method B blanks. Method A blanks contained MPs in the range of 12.5–16.7 items, with an average of 13.9 ± 2.4 MPs (Table S2). As a result, the LOD and LOQ of Method A blanks became 21.8 and 37.9 MPs per sample preparation, respectively. Method B blanks contained 0–1 MPs, which led to an average of 0.7 ± 0.6 MPs. Hence, the LOD and LOQ of blank B became 2.6 and 6.4 MPs per sample preparation, respectively. The LOD and LOQ calculations were based on the total number, even though the LOD and LOQ differed between polymer types, it was chosen only to calculate them for the total number of MPs as the numbers in the blanks were too low to yield meaningful LOD and LOQ values per polymer type.

It seemed that Method B had less contamination than Method A. However, Method A identified smaller MPs in its blanks than did Method B. The reason is partly that the instrument used in Method A had a lower size detection limit, and hence could identify smaller particles. The two methods also applied different wavenumber ranges, namely 3750–850 cm^{-1} (Method A) and 4000–1250 cm^{-1} (Method B). This means that Method A covered a larger part of the 'fingerprint' region, hence it potentially achieving a more secure identification.

3.1.2. MP concentration in River Danube

In the river water, Method A detected more smaller MPs, with MPs <50 μm accounting for around 30 % (Fig. 2(c-d)), despite the fact that the smallest sampling mesh size was 50 μm. These small MPs might be a result of aggregation and filter cake formation during sampling (Lorenz et al., 2019). Another possibility is that MPs break down during the isolation procedure because a magnetic stirrer was used to homogenise samples during processing. The stirring might, to some extent, have

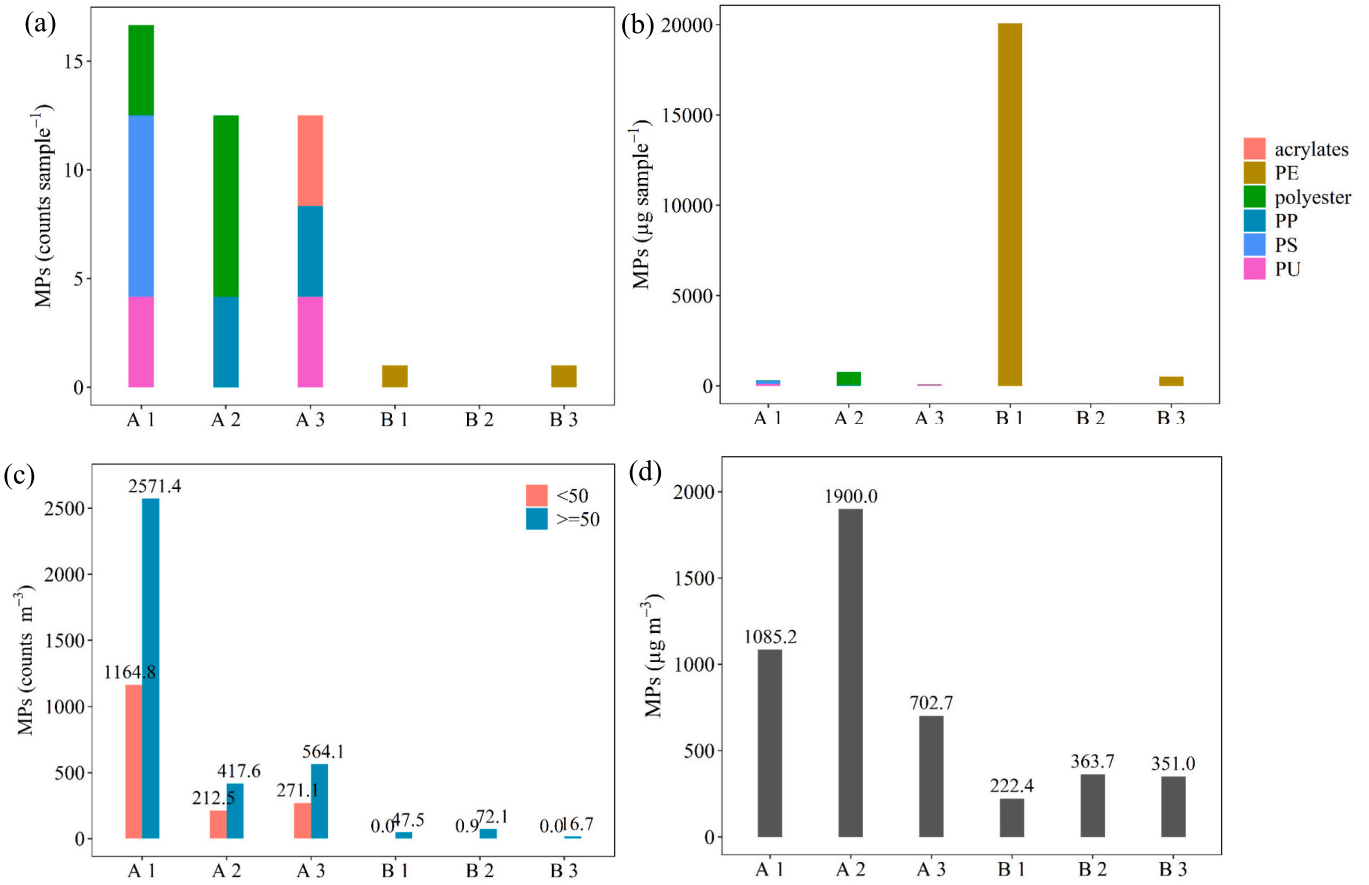

Fig. 2. (a) MP number and (b) MP mass concentration of Method A and B in Blanks. (c) MP number and (d) MP mass concentration estimates based on μFTIR analysis of Method A and B in Danube River water.

contributed to the breakdown of particles. Since sampled particles, in theory, should be >50 μm (based on the applied smallest mesh size), and to allow for better comparison between the instruments as they used different lower size detection limits, the following discussion is based on particles >50 μm (major dimension), unless otherwise explicitly stated. The LOD and LOQ in this size range became 13.49 and 29.61, respectively. Method A samples held 418–2571 counts m^{-3}, with an average of 1184 ± 1204 counts m^{-3} (Fig. 2(c)). This is significantly above what was reported in a previous study, which found a maximum of 141 counts m^{-3} in the Austrian part of the Danube (Lechner and Ramler, 2015). The difference can partly be explained by the size detection limit of that study (500 μm), and maybe also by differences in sample preparation and analysis. Method B detected a much lower abundance than Method A, namely 16.7–72.1 counts m^{-3}, with an average of 45.4 ± 27.7 counts m^{-3}. This means the MP abundance measured by Method A was 26 times above that of Method B, revealing significant differences in the outcome of the two methods. It is worth mentioning that a similar ratio was seen between Method A and B blanks.

The MP mass concentration determined by the two methods also showed some difference, but not as pronounced as for the MP abundance (Fig. 2(d)). This illustrates the necessity to include both number and mass concentrations when monitoring MPs in the environment. Just one measure does not yield the full picture. In summary, Method A held an MP mass of 703–1900 μg m^{-3}, with an average of 766 ± 615 μg m^{-3}, while Method B held an MP mass of 222–439 μg m^{-3}, with an average of 338 ± 109 μg m^{-3}. The mass concentration obtained by Method A was hence around 2.5 times higher than that of Method B. Such difference was also observed within methods, which indicated that the sample was not homogeneously separated. Still, the differences between methods were more pronounced than that within methods, which addressed the contribution of the method on the determination, a finding which also corresponds to the study of Simon-Sánchez et al. (2022).

3.1.3. Composition, size, and shape of MP

The distribution of MP polymer types in the Danube water differed when viewing the results as counts and mass (Fig. 3(a-b)). It also differed between the two methods. For the relative proportions of MP counts, PE dominated in Method A samples, while PP and PE dominated in Method B samples. The relative proportion of MP mass showed that PP dominated in Method A samples, while PVC dominated in Method B samples.

Size connects number and mass, as explained in Section 2.6, and size distribution can explain why number and mass data yielded different results. Most of the big particles, equalling large mass, were found in Method B samples (Fig. 3(c)). This means the same number of MPs in Method B samples weighted more than those of Method A, which can explain why less difference was found between mass concentrations than between number concentrations. This also indicated that Method B was better at extracting larger particles than smaller ones. The shape of the MPs – characterised as the ratio between major and minor Feret diameters – was similar between the methods (Fig. 3(d-e)), with fragments dominating for both.

A Principal Components Analysis (PCA) based on the major dimension, polymer type, mass, and shape (fibre, fragment), showed that there were overlaps between samples and methods (Fig. S1)). It showed that

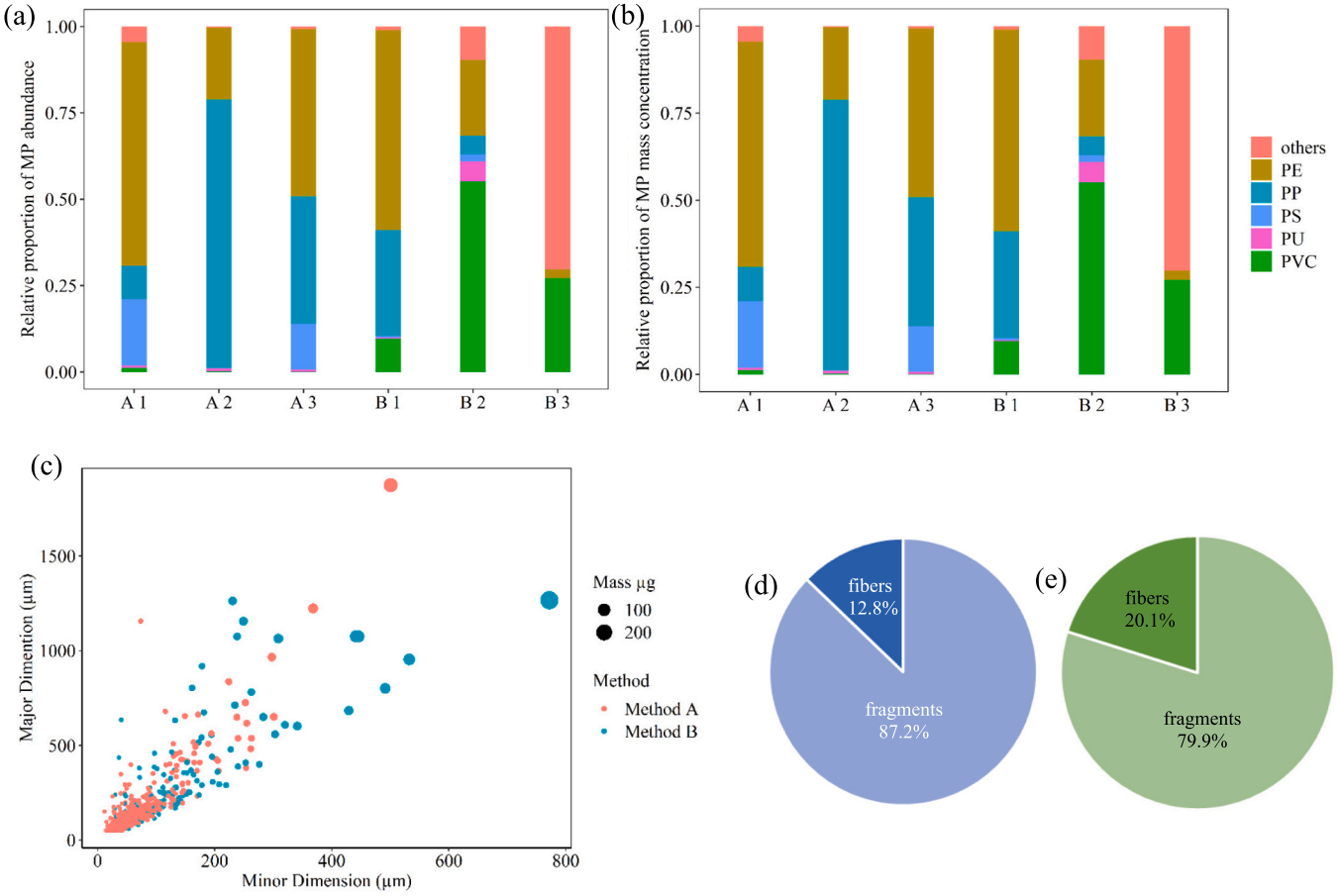

Fig. 3. Relative abundance of MP m^{-3} based on (a) abundance, (b) mass estimates based on μFTIR analysis of MP larger than 50 μm in Method A and B; (c) bubble plot representing minor vs major dimension of all detected MPs in Method A and B. Percentage of MP fibers and fragments for the total analysed samples of (d) Method A and (e) Method B. (All the calculation based on MPs (major dimension) > 50 μm).

the two methods led to differences in number and mass concentrations but not in MP characteristics (polymer type and particle shape).

To explain the difference between the methods, their individual steps, covering MP isolation procedures, substrates (ZnSe windows and Anodisc filters), and FTIR settings (pixel size and spectrum range) (Fig. S2), were examined. There were also more subtle differences between the procedures, for example, the number of coadded scans, and the number of scans used to create the background for the FTIR analysis. All these differences will affect the outcome of the analysis (Löder et al., 2015).

3.2. The effect of MP isolation

To explore the effect of MP isolation, recovery tests were conducted. As mentioned in Section 2.4.1, the beads were counted under an optical microscope illuminated with UV light, while the fragments were identified with μFTIR imaging. Comparing recovery rates of the beads versus fragments it must hence be considered that the beads covered the effect of the isolation procedures, while the fragments also covered the effect of substrates and FTIR settings. It furthermore turned out that the matrix for the recovery tests caused problems for Method B as the MCC (microcrystalline cellulose) was not digested and left a cake on the filters (Fig. S3). An additional cellulase step hence had to be included to allow these samples to be analysed (Löder et al., 2017).

In summary, Method A got a higher recovery rate than Method B, as shown in Table 2. For Method A, the bead recovery was 87 ± 2 %, and the difference in recovery rate between the two bead types was not statistically significant (85 ± 5 % and 88 ± 6 %, respectively), and had low standard deviation. PE fragments were recovered at a rate significantly above 100 % and with a quite high standard deviation (177 ± 62 %). PET fragments were recovered at rates like the PE beads but with a quite high standard deviation (83 ± 43 %). The increase in PE fragments might be caused by fragmentation (Löder and Gerdts, 2015), which also could explain the high standard deviation. It is though unclear what caused the high standard deviation for PET fragments. The substantial difference between fragment recovery and bead recovery shows that the type of standard particles and the identification technique might affect the assessment of a procedure's extraction efficiency. The overall recovery of beads, however, corresponded well with what Liu et al. (2023) found (90 ± 1 %) for marine waters using a similar procedure.

For Method B, the total beads recovery rate was 58 ± 4 %, which corresponded with what Mári et al. (2021) achieved (64 ± 29 %) for a similar method, using somewhat larger beads than the present study. However, here the recovery of fragments (42 ± 6 %) was lower than for beads.

The results indicated that the MP isolation procedure cannot explain all the differences between Danube samples analysed by the two methods (Fig. 2), but it is a significant contributor. The results also showed that some MPs will be lost during the MP isolation, which corresponds with what Isobe et al. (2019) found. Hence the MPs in the environment are likely underestimated. The bead recovery, done by stereo microscopy and hence not affected by potential biases caused by the FTIR analysis, was slightly better for Method A than B, and slightly more consistent. The difference was, however, not huge compared to the variability between individual samples (Fig. 2).

3.3. The effect of substrates

The substrate on which samples are scanned might affect the outcome of the analysis. On the Anodisc filters, 16.7–72.1 counts m^{-3} (average: 45.4 ± 27.7 counts m^{-3}) were found, while 175.8–332.8 counts m^{-3} (average: 247.7 ± 79.3 counts m^{-3}) were found on the ZnSe windows (Fig. 4(a) and (b)). For mass estimates, scanning on Anodisc filters yielded 222.4–439.3 μg m^{-3} (average: 337.6 ± 109.1 μg m^{-3}), while it on ZnSe windows yielded 151.2–646.2 μg m^{-3} (average: 300.8 ± 300.0 μg m^{-3}). Part of the reason why the mass was approx. The same on both substrates while the counts differed, was that the particles identified on the Anodisc filters appeared larger (Fig. 4(c)). Another part was caused by the mass estimation algorithm of siMPle, which assumes the thickness of the particles being proportional to the width of the equivalent ellipse (Simon et al., 2018). As volume and hence mass comes in the third power of particle dimension, a small increase in particle size leads to a large increase in estimated mass. A contributing factor for the fewer but larger particles identified on the Anodisc filters was that there was a higher tendency for particles, plastics, and natural ones, to agglomerate on the filters versus the ZnSe windows (pictures of the filters and windows are shown in Fig. S4). On the other hand, scanning with an FPA-FTIR on ZnSe windows tends to create an 'IR-halo' around a particle, making it seem larger than it is. This phenomenon is less pronounced for Anodisc filters.

As mentioned in Section 2.3, compared with the Anodisc filter, ZnSe windows only allow the scan of subsamples to avoid overlap between particles, and that subsampling for scanning will introduce an unknown uncertainty into the above discussions and conclusions. Nevertheless, it seems clear that the choice of substrate might well affect the quantification of MPs.

3.4. The effect of FTIR setting

The type of μFTIR imaging system and its settings also affect the results, as illustrated in Fig. 5(a). The windows prepared following Method A (windows 1–3) yielded 2–3 times more MP when scanned with the Cary FTIRs compared to the Nicolet FTIR, while the windows prepared following Method B (windows 4–6) yielded somewhat comparable results when scanned with the two systems. In further detail, windows 1, 2, 3, and 6 yielded more MPs when scanned by the Cary FTIR compared to the Nicolet FTIR, while the Nicolet FTIR yielded more MP mass for windows 2, 3, 4, and 5. These MP number and mass differences

Table 2
Recovery result for samples proceed with Method A and B isolation procedures.

	Spherical PE* (1.2 g cm^{-3})	Spherical PE* (0.98 g cm^{-3})	Spherical recovery rate	Fragment PE* (0.95 g cm^{-3})	Fragment PET**	Fragment recovery rate	Total recovery rate
A 1	18	17	88 %	32	25	143 %	115 %
A 2	17	17	85 %	49	17	165 %	125 %
A 3	16	19	88 %	25	8	83 %	85 %
Average rate	85 ± 5 %	88 ± 6 %	87 ± 2 %	177 ± 62 %	83 ± 43 %	130 ± 42 %	108 ± 21 %
B 1	14	9	58 %	3	3	15 %	36 %
B 2	10	12	55 %	11	3	35 %	45 %
B 3	12	13	63 %	12	0	30 %	46 %
Average rate	60 ± 10 %	57 ± 10 %	58 ± 4 %	43 ± 25 %	10 ± 9 %	27 ± 10 %	42 ± 6 %

The original number of each standard MPs per sample is 20 particles.
* PE - polyethylene.
** PET- polyethylene terephthalate.

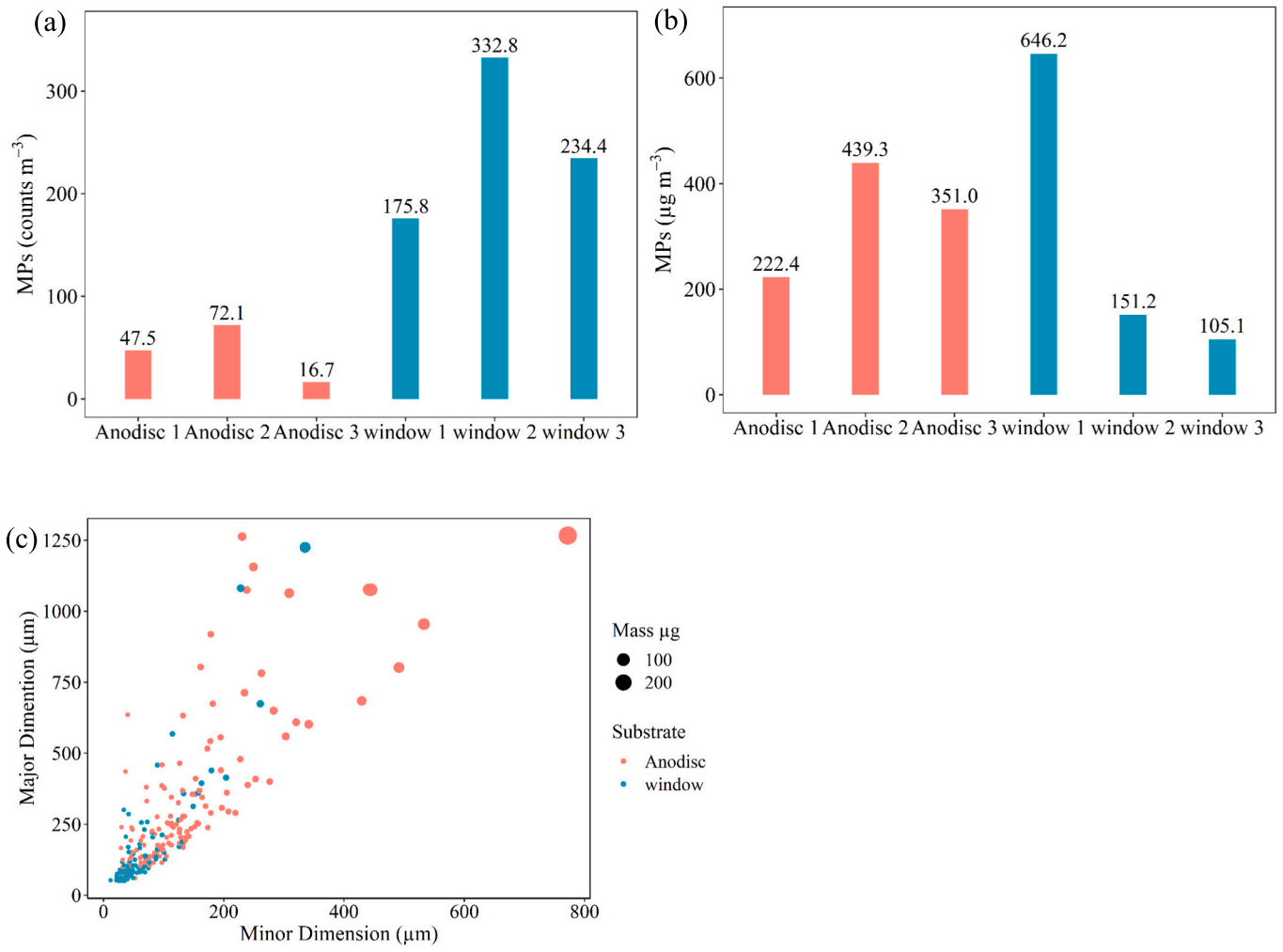

Fig. 4. (a) MP Abundance and (b) MP mass concentration of Method B using both Anodisc filter and windows. (c) size distribution of MPs detected on window and Anodisc filter. (All the calculation based on MPs (major dimension) > 50 µm. Same sample is labeled with same number, for example, Anodisc 1 and window 1 is the same sample).

might be related to the distribution of the particles on the windows, how crowded the windows were, and the potential overlap of particles. For windows 4–5, there was no big difference between the results obtained by the two systems, which might relate to the fact that only around 10 MPs were identified on each window and that they hence were quite well separated. However, for the windows with many MPs (windows 1–3 with around 100 MPs each), the MPs lay closer to each other, and the differences in pixel resolution of the two systems (5.5 µm versus 25 µm) made it more likely that two particles close to each other were identified as one. This also affects the mass estimate, as it assumes a thickness of the MP proportional to its size (Simon et al., 2018). As particle mass depends on the product of its three dimensions, one large particle of a certain area would hence yield a higher mass estimate than several smaller particles which together have that area. A further cause for potentially identifying particles as being larger (or smaller) than they are, is that particle size comes in steps related to the pixel resolution: The smaller the pixel size compared to the particle size, the more accurate the particle boundary can be defined.

3.5. Balancing pros and cons

It seems unlikely that any of the two methods yield the absolute truth of MP content in the samples. Neither would any other analytical method. They all give estimates and have advantages and disadvantages, as shown in Table 3. For the two investigated examples of methods, Method B was much more time- and cost-efficient, while Method A was more efficient at extracting MPs from the matrix. MP isolation by Method B took only 3 days, while Method A took 11 days (Fig. 1). Method B worked well in extracting MPs from the Danube water samples but poorly for the recovery test when adding MCC, indicating that Method B was inefficient at digesting cellulose, which could be an issue for other matrices. There were furthermore several large organic particles left after sample preparation (see Fig. S3 (a-c)), which potentially could have covered MPs and hereby hampered detection. All in all, Method B seemed to work well on comparatively simple matrices but was more prone to problems when addressing complex ones. Method A, on the other hand, worked well on complex matrices, which however came at the cost of being quite time-consuming. It also seemed to be somewhat harsher in terms of physically breaking down particles, a phenomenon that was observed in the recovery studies. For both methods, these issues can, of course, be addressed and solved, however, probably at some cost in terms of increased efforts to prepare and analyse the samples.

Regarding the choice of substrates, the Anodisc filter allowed flushing after deposition, and could hence better manage dissolved residues in the extracts than could the windows. Additionally, these

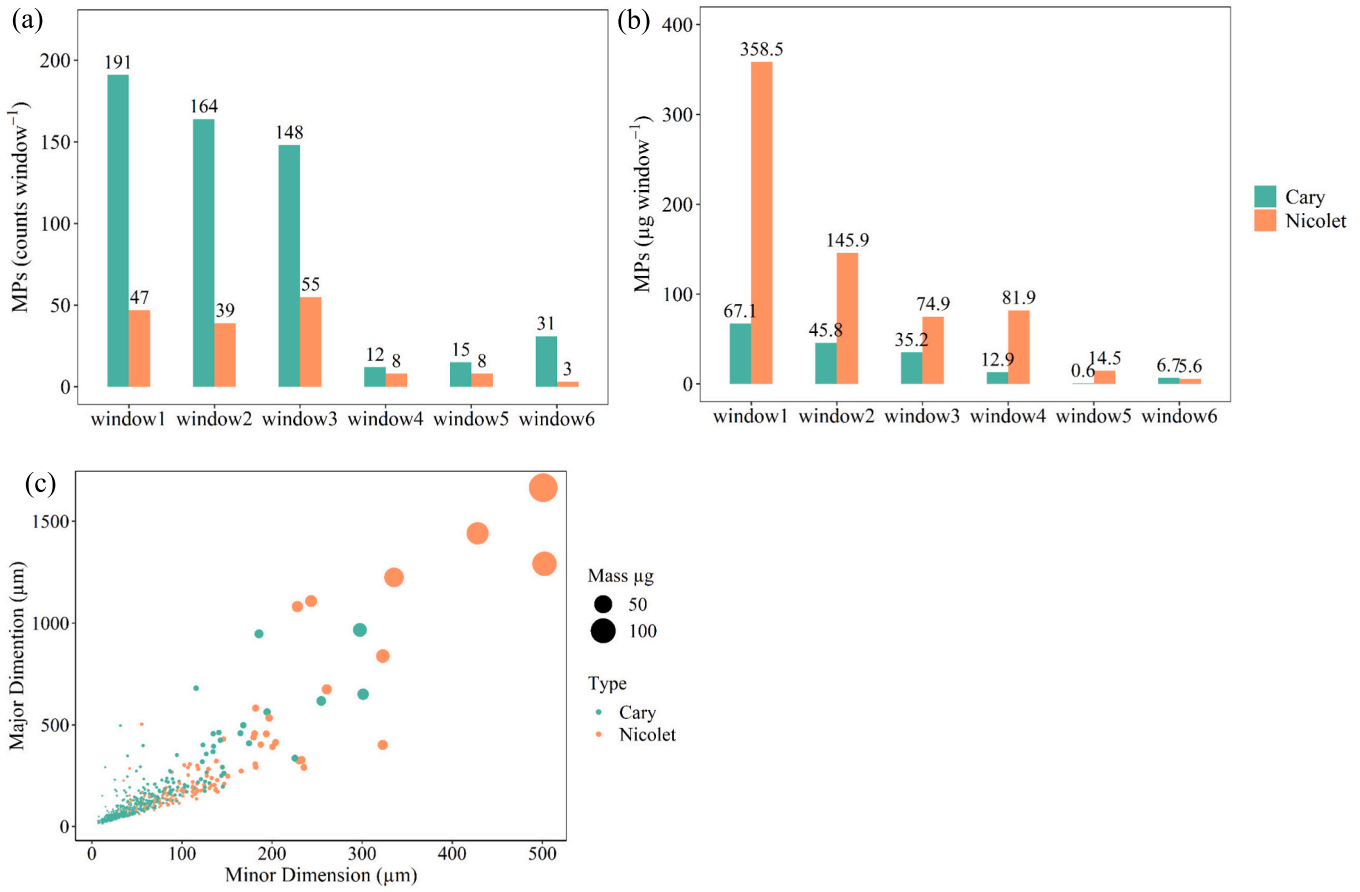

Fig. 5. (a) MP abundance and (b) MP mass concentration on window by both Nicolet and Cary FTIR microscope based on the MP number and mass (window 1–3: Method A sample; window 4–6: Method B samples). (c) size distribution of MPs detected with Nicolet and Cary FTIR microscope. (This discussion covers all size range).

filters possess relatively small pore sizes (maximum 0.2 µm), leading to lower filtration velocity and the retention of particles smaller than the IR detection limit. Nevertheless, the advantage lies in their cost-effectiveness, rendering them well-suited for conducting comprehensive studies with a large number of samples (Primpke et al., 2020a; Ivleva, 2021). Scanning on windows requires more rigorous removal of dissolved residuals in the concentrates. The issue of particle crowding remained the same for both substrates, as it was a question of ensuring separation between particles. A drawback of the Anodisc filter was that it only allows analysing the wavenumber range 4000–1250 cm^{-1}, which meant that part of the fingerprint range was lost (Löder et al., 2015; Primpke et al., 2019). The windows, on the other hand, allowed a broader range, 3750–850 cm^{-1}, to be scanned (Liu et al., 2023). Regarding the FTIR machine itself and its setting, a lower spatial resolution allowed a more precise MP identification, including more MPs to be identified. However, the imaging system with the higher spatial resolution is also the more expensive one.

The two methods clearly differ, and which to choose will depend on a multitude of factors. Should one go for the simpler and less costly approach or for the more complex and resource-demanding approach? Do gained data quality benefits justify the increased costs? Sometimes the answer will be a yes, sometimes a no. However, what is not up for debate is that different analytical methods will yield different results. This indicates a strong need for harmonization and standardisation in the field of MP sampling and analysis.

4. Conclusion

This study investigated the impact of different MP analysis procedures and analytical techniques on the quantification of MPs in the environment. Two representative methods were applied to analyze samples collected from the Danube River, and the results highlighted the significant contribution of various steps (such as MP isolation procedures, substrate, and FTIR settings) to the outcomes. The results showed that Method A yielded a higher number and mass concentration of MPs, while Method B was found to be more time- and cost-efficient. The study showed that the procedures used can affect the numerical results, and the effect of individual steps can vary from sample to sample. The findings suggest that the MP isolation procedure can influence MP morphology and lead to the loss of particles during the isolation procedure. For substrates, it can be concluded that the samples could be analysed on the Anodisc filter in the wavenumber range of 4000–1250 cm^{-1} without interference with chemical residuals, while only subsamples could be deposited on ZnSe window, which then were analysed in the wavenumber range of 3750–850 cm^{-1}. In other words, this substrate required more rigorous removal of dissolved residuals from the concentrates. The study also found that different FTIR settings (pixel size) can affect the size and number of MPs, and that smaller pixel sizes results in easier identification of the real outline of MPs. All these findings address the contribution of the analytical methodology to our understanding of MPs in the environment and highlight the necessity to work towards harmonised methodologies to increase comparability among studies.

Table 3
Pros and cons of Method A and B.

	Method		
	A	B	
Time needed for analysis	−	+	Method A required about 12 working days for a full analysis, while Method B made do with 4 working days.
Chemicals required	−	+	Method A needed at least one chemical in each step, including different enzymes, H_2O_2, $FeSO_4$, NaOH, $ZnCl_2$, and EtOH, while Method B only needed H_2O_2, $ZnCl_2$ and HCl.
Efficiency in organic matter degradation	+++	−	Method A could remove most organic matters, while Method B was limited in removing organic matters.
Recovery rate of MP isolation procedure	++	+	Both methods achieved a stable recovery rate of reference beads, and the recovery rate of Method A was higher than Method B.
Substrate transmissivity	+++	+	The ZnSe window could cover most wavenumbers of the fingerprint area, and covered 3750–850 cm^{-1}, while the Anosic filter could only cover 4000–1250 cm^{-1}.
Substrate loading	+	++	The ZnSe window only allowed the detection of subsamples, while the Anodisc filter could load the whole sample.
Residual chemicals left on the substrate	+	++	Anodisc filters were not prone to dissolve residual chemicals as these can be washed out. ZnSe windows, on the other hand, were rather sensitive to residual chemicals as they stayed on the window where they could hamper the analysis.
Particle distribution	++	+	Particles distributed well on ZnSe windows and while they overcrowded the Anodisc filter.
FTIR detection limit	+++	+	The detection limit of the Cary FTIR was 11 μm, while that of the Nicolet FTIR was 50 μm.

CRediT authorship contribution statement

Yuanli Liu: Writing – Original draft preparation, Experimental section, and Visualization; Bence Prikler – Sampling, Experiment section, Writing – Reviewing and Editing; Gábor Bordós – Supervision, Sampling, Writing- Reviewing and Editing; Claudia Lorenz: Supervision, Writing – Reviewing and Editing; Jes Vollertsen: Supervision, Funding acquisition; Writing – Reviewing and Editing.

Declaration of competing interest

The authors declare that they have no known competing financial interests or personal relationships that could have appeared to influence the work reported in this paper.

Data availability

Data will be made available on request.

Acknowledgments

This project was funded by MONPLAS (European Union's Horizon 2020 research and innovation programme under the Marie Skłodowska-Curie grant agreement No 860775. H2020-MSCA-ITN-2019). We would also appreciate the support from Eurofins Analytical Services Hungary Ltd. for this great cooperation.

Appendix A. Supplementary data

Supplementary data to this article can be found online at https://doi.org/10.1016/j.scitotenv.2023.166513.

References

Bannick, C.G., Szewzyk, R., Ricking, M., Schniegler, S., Obermaier, N., Barthel, A.K., Altmann, K., Eisentraut, P., Braun, U., 2019. Development and testing of a fractionated filtration for sampling of microplastics in water. Water Res. 149, 650–658. https://doi.org/10.1016/J.WATRES.2018.10.045.

Bäuerlein, P.S., Hofman-Caris, R., Pieke, E.N., ter Laak, L., T., 2022. Fate of microplastics in the drinking water production. Water Res. 118790 https://doi.org/10.1016/J.WATRES.2022.118790.

Bertoldi, C., Lara, L.Z., de L. Mizushima, F.A., Martins, F.C.G., Battisti, M.A., Hinrichs, R., Fernandes, A.N., 2021. First evidence of microplastic contamination in the freshwater of Lake Guaíba, Porto Alegre, Brazil. Sci. Total Environ. 759, 143503 https://doi.org/10.1016/J.SCITOTENV.2020.143503.

Blettler, M.C.M., Abrial, E., Khan, F.R., Sivri, N., Espinola, L.A., 2018. Freshwater plastic pollution: recognizing research biases and identifying knowledge gaps. Water Res. 143, 416–424. https://doi.org/10.1016/j.watres.2018.06.015.

Bordós, G., Gergely, S., Háhn, J., Palotai, Z., Szabó, É., Besenyő, G., Salgó, A., Harkai, P., Kriszt, B., Szoboszlay, S., 2021. Validation of pressurized fractionated filtration microplastic sampling in controlled test environment. Water Res. 189, 116572 https://doi.org/10.1016/J.WATRES.2020.116572.

Chand, R., Rasmussen, L.A., Tumlin, S., Vollertsen, J., 2021. The occurrence and fate of microplastics in a mesophilic anaerobic digester receiving sewage sludge, grease, and fatty slurries. Sci. Total Environ. 798, 149287 https://doi.org/10.1016/J.SCITOTENV.2021.149287.

Cole, M., 2016. A novel method for preparing microplastic fibers. Scientific Reports 2016 6:1 6 (1), 1–7. https://doi.org/10.1038/srep34519.

Corami, F., Rosso, B., Bravo, B., Gambaro, A., Barbante, C., 2020. A novel method for purification, quantitative analysis and characterization of microplastic fibers using Micro-FTIR. Chemosphere 238, 124564. https://doi.org/10.1016/J.CHEMOSPHERE.2019.124564.

Corradini, F., Casado, F., Leiva, V., Huerta-Lwanga, E., Geissen, V., 2021. Microplastics occurrence and frequency in soils under different land uses on a regional scale. Sci. Total Environ. 752, 141917 https://doi.org/10.1016/j.scitotenv.2020.141917.

Eo, S., Hong, S.H., Song, Y.K., Han, G.M., Shim, W.J., 2019. Spatiotemporal distribution and annual load of microplastics in the Nakdong River, South Korea. Water Res. 160, 228–237. https://doi.org/10.1016/J.WATRES.2019.05.053.

Eo, S., Hong, S.H., Song, Y.K., Han, G.M., Seo, S., Shim, W.J., 2021. Prevalence of small high-density microplastics in the continental shelf and deep sea waters of East Asia. Water Res. 200, 117238 https://doi.org/10.1016/J.WATRES.2021.117238.

González, D., Hanke, G., Tweehuysen, G., Bellert, B., Holzhauer, M., Palatinus, A., Hohenblum, P., Oosterbaan, L., 2016. Riverine litter monitoring - options and recommendations. MSFD GES TG marine litter thematic report. JRC Technical Report EUR 28307. https://doi.org/10.2788/461233.

Horton, A.A., Cross, R.K., Read, D.S., Jürgens, M.D., Ball, H.L., Svendsen, C., Vollertsen, J., Johnson, A.C., 2021. Semi-automated analysis of microplastics in complex wastewater samples. Environ. Pollut. 268, 115841 https://doi.org/10.1016/J.ENVPOL.2020.115841.

Huang, W., Song, B.A., Liang, J., Niu, Q.Y., Zeng, G.M., Shen, M.C., Deng, J.Q., Luo, Y.A., Wen, X.F., Zhang, Y.F., 2021. Microplastics and associated contaminants in the aquatic environment: A review on their ecotoxicological effects, trophic transfer, and potential impacts to human health. J. Hazard. Mater. 405, 124187 https://doi.org/10.1016/j.jhazmat.2020.124187.

Huang, Z.K., Hu, B., Wang, H., 2023. Analytical methods for microplastics in the environment: a review. Environ. Chem. Lett. 21, 383–401. https://doi.org/10.1007/s10311-022-01525-7.

Isobe, A., Buenaventura, T.N., Chastain, S., Chavanich, S., Cózar, A., DeLorenzo, M., Hagmann, P., Hinata, H., Kozlovskii, N., Lusher, L.A., Martí, Elisa, Michida, Y., Mu, J., Ohno, M., Potter, G., Ross, S.P., Sagawa, N., Shim, W.J., Song, Y.K., Takada, H., Tokai, T., Torii, T., Uchida, K., Vassillenko, K., Viyakarn, V., Zhang, W. W., 2019. An interlaboratory comparison exercise for the determination of microplastics in standard sample bottles. Mar. Pollut. Bull. 146, 831–837. https://doi.org/10.1016/j.marpolbul.2019.07.033.

Ivleva, P.V., 2021. Chemical analysis of microplastics and nanoplastics: challenges, advanced methods, and perspectives. Chem. Rev. 121, 11886–11936. https://doi.org/10.1021/acs.chemrev.1c00178.

Jiang, C., Yin, L., Li, Z., Wen, X., Luo, X., Hu, S., Yang, H., Long, Y., Deng, B., Huang, L., Liu, Y., 2019. Microplastic pollution in the rivers of the Tibet plateau. Environ. Pollut. 249, 91–98. https://doi.org/10.1016/J.ENVPOL.2019.03.022.

Kappler, A., Windrich, F., Loder, M.G.J., Malanin, M., Fischer, D., Labrenz, M., Eichhorn, K.J., Voit, B., 2015. Identification of microplastics by FTIR and Raman microscopy: a novel silicon filter substrate opens the important spectral range below 1300 cm^{-1} for FTIR transmission measurements. Anal. Bioanal. Chem. 407, 6791–6801. https://doi.org/10.1007/s00216-015-8850-8.

Katsumi, N., Nagao, S., Okochi, H., 2022. Addition of polyvinyl pyrrolidone during density separation with sodium iodide solution improves recovery rate of small microplastics (20-150 μm) from soils and sediments. Chemosphere 307 (Part 1), 135730. https://doi.org/10.1016/j.chemosphere.2022.135730.

Khalid, N., Aqeel, M., Noman, A., Hashem, M., Mostafa, Y.S., Alhaithloul, H.A.S., Alghanem, S.M., 2021. Linking effects of microplastics to ecological impacts in marine environments. Chemosphere 264 (Part 2), 128541. https://doi.org/10.1016/j.chemosphere.2020.128541.

Kirstein, I.V., Hensel, F., Gomiero, A., Iordachescu, L., Vianello, A., Wittgren, H.B., Vollertsen, J., 2021. Drinking plastics? – quantification and qualification of

microplastics in drinking water distribution systems by μFTIR and Py-GCMS. Water Res. 188, 116519 https://doi.org/10.1016/J.WATRES.2020.116519.
Lechner, A., Ramler, D., 2015. The discharge of certain amounts of industrial microplastic from a production plant into the River Danube is permitted by the Austrian legislation. Environ. Pollut. 200, 159–160. https://doi.org/10.1016/j.envpol.2015.02.019.
Lin, L., Zuo, L.Z., Peng, J.P., Cai, L.Q., Fok, L., Yan, Y., Li, H.X., Xu, X.R., 2018. Occurrence and distribution of microplastics in an urban river: A case study in the Pearl River along Guangzhou City, China. Sci. Total Environ. 644, 375–381. https://doi.org/10.1016/J.SCITOTENV.2018.06.327.
Liu, F., Olesen, K.B., Borregaard, A.R., Vollertsen, J., 2019a. Microplastics in urban and highway stormwater retention ponds. Sci. Total Environ. 671, 992–1000. https://doi.org/10.1016/J.SCITOTENV.2019.03.416.
Liu, F., Vianello, A., Vollertsen, J., 2019b. Retention of microplastics in sediments of urban and highway stormwater retention ponds. Environ. Pollut. 255, 113335 https://doi.org/10.1016/J.ENVPOL.2019.113335.
Liu, Y., Lorenz, C., Vianello, A., Syberg, K., Nielsen, H.A., Nielsen, Torkel Gissel, Vollertsen, Jes, 2023. Exploration of occurrence and sources of microplastics (>10 μm) in Danish marine waters. Sci. Total Environ. 865, 161255. ISSN 0048-9697. https://doi.org/10.1016/j.scitotenv.2022.161255.
Löder, M.G.J., Gerdts, G., 2015. Methodology used for the detection and identification of microplastics—A critical appraisal. In: Bergmann, M., Gutow, L., Klages, M. (Eds.), Marine Anthropogenic Litter. Springer International Publishing, pp. 201–227. https://link.springer.com/chapter/10.1007/978-3-319-16510-3_8#copyright-information.
Löder, M.G.J., Kuczera, M., Mintenig, S., Lorenz, C., Gerdts, G., Löder, M.G.J., Kuczera, M., Mintenig, S., Lorenz, C., Gerdts, G., 2015. Focal plane array detector-based micro-Fourier-transform infrared imaging for the analysis of microplastics in environmental samples. Environ. Chem. 12 (5), 563–581. https://doi.org/10.1071/EN14205.
Löder, M.G.J., Imhof, H.K., Ladehoff, M., Löschel, L.A., Lorenz, C., Mintenig, S., Piehl, S., Primpke, S., Schrank, I., Laforsch, C., Gerdts, G., 2017. Enzymatic purification of microplastics in environmental samples. Environ. Sci. Technol. 51 (24), 14283–14292. https://doi.org/10.1021/ACS.EST.7B03055/SUPPL_FILE/ES7B03055_SI_001.PDF.
Lorenz, C., Roscher, L., Meyer, M.S., Hildebrandt, L., Prume, J., Löder, M.G.J., Primpke, S., Gerdts, G., 2019. Spatial distribution of microplastics in sediments and surface waters of the southern North Sea. Environ. Pollut. 252, 1719–1729. https://doi.org/10.1016/j.envpol.2019.06.093.
Lusher, A.L., Munno, K., Hermabessiere, L., Carr, S., 2020. Isolation and extraction of microplastics from environmental samples: an evaluation of practical approaches and recommendations for further harmonization. Appl. Spectrosc. 74 (9), 1049–1065. https://doi.org/10.1177/0003702820938993.
Mănoiu, V.M., Crăciun, A.I., 2021. Danube river water quality trends: A qualitative review based on the open access web of science database. Ecohydrol. Hydrobiol. 21 (4), 613–628. https://doi.org/10.1016/J.ECOHYD.2021.08.002.
Mári, Á., Bordós, G., Gergely, S., Büki, M., Háhn, J., Palotai, Z., Besenyő, G., Szabó, É., Salgó, A., Kriszt, B., Szoboszlay, S., 2021. Validation of microplastic sample preparation method for freshwater samples. Water Res. 202, 117409 https://doi.org/10.1016/J.WATRES.2021.117409.
McIlwraith, H.K., Kim, J., Helm, P., Bhavsar, S.P., Metzger, J.S., Rochman, C.M., 2021. Evidence of microplastic translocation in wild-caught fish and implications for microplastic accumulation dynamics in food webs. Environ. Sci. Technol. 55 (18), 12372 https://doi.org/10.1021/acs.est.1c02922.
Molazadeh, M., Liu, F., Simon-Sánchez, L., Vollersten, J., 2023. Buoyant microplastics in freshwater sediments – how do they get there? Sci. Total Environ. 860, 160489 https://doi.org/10.1016/j.scitotenv.2022.160489.
van Mourik, L.M., Crum, S., Martinez-Frances, E., van Bavel, B., Leslie, H.A., de Boer, J., Cofino, W.P., 2021. Results of WEPAL-QUASIMEME/NORMANs first global interlaboratory study on microplastics reveal urgent need for harmonization. Sci. Total Environ. 772, 145071 https://doi.org/10.1016/j.scitotenv.2021.145071.
Nizamali, J., Mintenig, S.M., Koelmans, A.A., 2022. Assessing microplastic characteristics in bottled drinking water and air deposition samples using laser direct infrared imaging. J. Hazard. Mater. 129942 https://doi.org/10.1016/J.JHAZMAT.2022.129942.
Phuong, N.N., Fauvelle, V., Grenz, C., Ourgaud, M., Schmidt, N., Strady, E., Sempere, R., 2021. Highlights from a review of microplastics in marine sediments. Sci. Total Environ. 777, 146225 https://doi.org/10.1016/j.scitotenv.2021.146225.
Possenti, E., Colombo, C., Realini, M., Song, C.L., Kazarian, S.G., 2021. Time-resolved ATR-FTIR spectroscopy and macro ATR-FTIR spectroscopic imaging of inorganic treatments for stone conservation. Anal. Chem. 93 (44), 14635–14642. https://doi.org/10.1021/acs.analchem.1c02392.
Prepilkova, V., Ponist, J., Schwarz, M., Bednarova, D., 2022. Selection of suitable methods for the detection of microplastics in the environment. J. Anal. Chem. 77, 830–843. https://doi.org/10.1134/S1061934822070127.
Primpke, S., Lorenz, C., Rascher-Friesenhausen, R., Gerdts, G., 2017a. An automated approach for microplastics analysis using focal plane array (FPA) FTIR microscopy and image analysis. Anal. Methods 9, 1499. https://doi.org/10.1039/c6ay02476a.
Primpke, S., Lorenz, C., Rascher-Friesenhausen, R., Gerdts, G., 2017b. An automated approach for microplastics analysis using focal plane array (FPA) FTIR microscopy and image analysis. Anal. Methods 9, 1499–1511. https://doi.org/10.1039/c6ay02476a.
Primpke, S., Dias, P.A., Gerdts, G., 2019. Automated identification and quantification of microfibres and microplastics. Anal. Methods 11, 2138–2147. https://doi.org/10.1039/C9AY00126C.
Primpke, S., Christiansen, S.H., Cowger, W., De Frond, H., Deshpande, A., Fischer, M., Holland, E.B., Meyns, M., O'Donnell, B.A., Ossmann, B.E., Pittroff, M., Sarau, G., Scholz-Bottcher, B.M., Wiggin, K.J., 2020a. Critical assessment of analytical methods for the harmonized and cost-efficient analysis of microplastics. Appl. Spectrosc. 74 (9), 1012–1047. https://doi.org/10.1177/0003702820921465.
Primpke, S., Cross, R.K., Mintenig, S.M., Simon, M., Vianello, A., Gerdts, G., Vollertsen, J., 2020b. Toward the systematic identification of microplastics in the environment: evaluation of a new independent software tool (siMPle) for spectroscopic analysis. Appl. Spectrosc. 74 (9), 1127–1138. https://doi.org/10.1177/0003702820917760.
Rahman, A., Sarkar, A., Yadav, O.P., Achari, G., Slobodnik, J., 2021. Potential human health risks due to environmental exposure to nano- and microplastics and knowledge gaps: A scoping review. Sci. Total Environ. 757, 143872 https://doi.org/10.1016/j.scitotenv.2020.143872.
Rezaei, M., Abbasi, S., Pourmahmood, H., Oleszczuk, P., Ritsema, C., Turner, A., 2022. Microplastics in agricultural soils from a semi-arid region and their transport by wind erosion. Environ. Res. 212, 113213 https://doi.org/10.1016/J.ENVRES.2022.113213.
Rist, S., Vianello, A., Winding, M.H.S., Nielsen, T.G., Almeda, R., Torres, R.R., Vollertsen, J., 2020. Quantification of plankton-sized microplastics in a productive coastal Arctic marine ecosystem. Environ. Pollut. 266, 115248 https://doi.org/10.1016/J.ENVPOL.2020.115248.
Simon, M., van Alst, N., Vollertsen, J., 2018. Quantification of microplastic mass and removal rates at wastewater treatment plants applying focal plane Array (FPA)-based Fourier transform infrared (FT-IR) imaging. Water Res. 142, 1–9. https://doi.org/10.1016/J.WATRES.2018.05.019.
Simon-Sánchez, L., Grelaud, M., Franci, M., Ziveri, P., 2022. Are research methods shaping our understanding of microplastic pollution? A literature review on the seawater and sediment bodies of the Mediterranean Sea. Environ. Pollut. 292, 118275 https://doi.org/10.1016/J.ENVPOL.2021.118275.
Song, Y.K., Hong, S.H., Jang, M., Han, G.M., Rani, M., Lee, J., Shim, W.J., 2015. A comparison of microscopic and spectroscopic identification methods for analysis of microplastics in environmental samples. Mar. Pollut. Bull. 93 (1–2), 202–209. https://doi.org/10.1016/J.MARPOLBUL.2015.01.015.
Thomas, D., Schutze, B., Heinze, W.M., Steinmetz, Z., 2020. Sample preparation techniques for the analysis of microplastics in soil—A review. Sustainability 12 (21), 9074. https://doi.org/10.3390/su12219074.
Tirkey, A., Upadhyay, L.S.B., 2021. Microplastics: an overview on separation, identification and characterization of microplastics. Mar. Pollut. Bull. 170, 112604 https://doi.org/10.1016/j.marpolbul.2021.112604.
Valls-Conesa, J., Winterauer, D.J., Kröger-Lui, N., Roth, S., Liu, F., Lüttjohann, S., Hariga, R., Vollertsen, J., 2023. Random forest microplastic classification using spectral subsamples of FT-IR hyperspectral images. Anal. Methods 15, 2226. https://doi.org/10.1039/d3ay00514c.
Wander, L., Vianello, A., Vollertsen, J., Westad, F., Braun, U., Paul, A., 2020. Exploratory analysis of hyperspectral FTIR data obtained from environmental microplastics samples. Anal. Methods 12, 781–791. https://doi.org/10.1039/C9AY02483B.
Wang, G., Lu, J., Tong, Y., Liu, Z., Zhou, H., Xiayihazi, N., 2020. Occurrence and pollution characteristics of microplastics in surface water of the Manas River basin, China. Sci. Total Environ. 710, 136099 https://doi.org/10.1016/J.SCITOTENV.2019.136099.
Weber, F., Kerpen, J., 2022. Underestimating microplastics? Quantification of the recovery rate of microplastic particles including sampling, sample preparation, subsampling, and detection using μ-Ramanspectroscopy. Anal. Bioanal. Chem. https://doi.org/10.1007/s00216-022-04447-z.
Xiong, X., Tappenbeck, T.H., Wu, C., Elser, J.J., 2022. Microplastics in Flathead Lake, a large oligotrophic mountain lake in the USA. Environ. Pollut. 306, 119445 https://doi.org/10.1016/J.ENVPOL.2022.119445.
Ye, Y., Yu, K., Zhao, Y., 2022. The development and application of advanced analytical methods in microplastics contamination detection: A critical review. Sci. Total Environ. 818, 151851 https://doi.org/10.1016/J.SCITOTENV.2021.151851.
Yin, L., Wen, X., Huang, D., Zhou, Z., Xiao, R., Du, L., Su, H., Wang, K., Tian, Q., Tang, Z., Gao, L., 2022. Abundance, characteristics, and distribution of microplastics in the Xiangjiang river, China. Gondwana Res. 107, 123–133. https://doi.org/10.1016/J.GR.2022.01.019.
Yuan, Z., Nag, R., Cummins, E., 2022. Ranking of potential hazards from microplastics polymers in the marine environment. J. Hazard. Mater. 429, 128399 https://doi.org/10.1016/J.JHAZMAT.2022.128399.
Zhang, Y., Peng, Y., Xu, S., Zhang, S., Zhou, G., Yang, J., Li, H., Zhang, J., 2022. Distribution characteristics of microplastics in urban rivers in Chengdu city: the influence of land-use type and population and related suggestions. Sci. Total Environ. 846, 157411 https://doi.org/10.1016/J.SCITOTENV.2022.157411.
Zhou, G., Wang, Q., Zhang, J., Li, Q., Wang, Y., Wang, M., Huang, X., 2020. Distribution and characteristics of microplastics in urban waters of seven cities in the Tuojiang River basin, China. Environ. Res. 189, 109893 https://doi.org/10.1016/J.ENVRES.2020.109893.